

# Thermal Dose Optimization Via Temporal Switching in Ultrasound Surgery

Douglas R. Daum and Kullervo Hynynen

**Abstract**—Temporal switching has been simulated and implemented in vivo experiments as a method to optimize thermal dose in ultrasound surgery. By optimizing the thermal dose over a tissue volume, the peak temperature is decreased, less average power is expended, and overall treatment time is shortened. To test this hypothesis, a 16 element, spherically sectioned array has been constructed for application in ultrasound surgery guided by magnetic resonance imaging. A simulation study for the array was performed to determine an optimal treatment from a set of multiple focus fields. These fields were generated using the mode scanning technique with power levels determined numerically using a direct weighted gradient search in the attempt to create an optimally uniform thermal dose over a  $0.6 \times 0.6 \times 1.0 \text{ cm}^3$  tissue volume. Comparisons of the switched fields and a static multiple focus field indicate that the switching technique can lower power requirements and decrease treatment time by 20%. More importantly, the peak temperature of the sonication was lowered  $13^\circ\text{C}$ , thus decreasing the possibility of cavitation. The simulated results of the 16 element array were then experimentally tested using MRI to noninvasively monitor temperature elevations and predict lesion size in rabbit thigh muscle in vivo. In addition, the results show that the switching technique can be less sensitive to tissue inhomogeneities than static field sonication while creating contiguous necrosis regions at equal average powers.

## I. INTRODUCTION

Therapeutic phased array ultrasound transducers are advantageous in the treatment of large tumors because they are capable of generating larger lesions than their non-phased counterparts [1]–[5]. The creation of these lesions is possible through the use of multiple focus intensity patterns which distribute power and create temperature elevations over regions much larger than those from a single spot focus. For multiple focus therapy to be successful, however, care must be taken to reduce near field heating [3], [6], [7] and secondary temperature elevations [2]. An earlier study demonstrated that the rate limiting factors to necrose large tumors include both the deposition of power in the tumor volume and the cooling period necessary between sonications [3]. If proper cooling times are not used, sequential sonications could damage prefocal tissue [4]–[7] or be blocked by thermally induced cavitation between the transducer and the tumor volume [7]–[10]. Thus, although

Manuscript received March 18, 1997; accepted July 29, 1997. This research was done under NIH Grant CA46627. The authors thank GE Medical Systems for the temperature imaging sequences and positional equipment.

The authors are with Department of Radiology, Brigham and Women's Hospital, and Harvard Medical School, Boston, MA 02115.

multiple focus patterns have been shown to yield faster necrosis rates than single focus sonications, the phased array treatments may still require extensive cooling times to produce a continuous necrosed tissue volume [5], [11].

To shorten the treatment duration and improve performance of phased array ultrasound surgery, this research investigates a method to rapidly switch between multiple focus patterns such that the thermal response of the array is more uniform, thus lowering peak temperatures using less average acoustic output power. This technique is similar to the temporal switching simulated for hyperthermia treatment [12], [13], but differs in several key aspects. First, this switching technique is designed for the short duration sonications required in ultrasound surgery. Therefore, an important consideration for implementing this technique is the rate at which the patterns are switched. Second, the primary goal of this research is to increase the tissue treatment volume rate without producing undesirable therapeutic conditions. These conditions include excessively elevated temperatures in the tissue and high transducer output power. Third, while previous research has simulated and tested temporal switching in a water bath, this research experimentally tests a temporal switching technique in vivo for ultrasound surgery using temperature sensitive mapping provided by noninvasive magnetic resonance imaging (MRI) [15].

## II. METHODS AND MATERIALS

### A. Phased Array Design

A spherically sectioned array introduced by Ebbini and Cain [16] and similar to the one described by Fan and Hynynen [3] was designed and constructed for application in MRI guided surgery (Fig. 1). The array had 16 elements, was sectioned from a single PZT-4 polycrystal, and was matched to  $50 \Omega$  near its resonance at 1.64 MHz using simple inductor-capacitor circuitry. The array was powered by a newly constructed phased array driving system with 8-bit phase resolution and self leveling 0-60 W/channel power control.

### B. Acoustic Measurements

The elements yielded acoustical efficiencies ranging from 70% to 80% at 2.5 to 3.5 W/cm<sup>2</sup> as measured by a radiation force technique [17]. Beam plots in a water bath were measured using a thermistor with a 0.25 mm

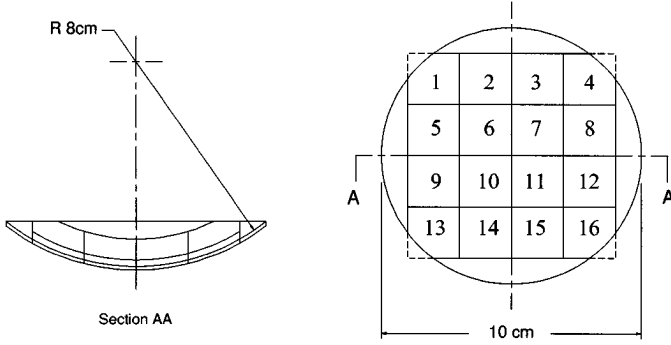


Fig. 1. Spherically shaped square element array geometry.

silicone bead or by using a 0.5 mm hydrophone (NTR, Seattle, WA).

C. Numerical Simulation

Throughout this research, ultrasound fields were simulated using the Rayleigh-Sommerfeld integral over a set of geometrically superimposed point sources as described by Zemanek [18]. The temperature elevations were calculated numerically using the Pennes bio-heat transfer equation [19], and the dose distributions were calculated from a numerical integration of the Sapareto and Dewey model [20]. In all simulations, the spatial resolution was at least 0.25 mm in the transverse axis and 0.50 mm in the longitudinal axis and the temporal resolution was smaller than 0.02 s. All calculations were performed on a multiprocessor IBM PVS computer.

D. Optimization Routine

The goal of the optimization routine was to create a uniform dose over a region of interest during a single sonication time period. To accomplish this, six patterns which covered the possible region of sonication for the given array geometry were chosen as inputs to the power optimization routine (Fig. 2). The driving signals for these patterns were calculated using the mode scanning technique which reduces near field heating by causing destructive interference along different axial planes of the transducer [1], [12], [21]. For example, pattern (b) of Fig. 2 was created by driving all of the elements with equal amounts of power, but by varying their phases with rotational symmetry. In this case, the center 4 elements (clockwise) are driven with phases of  $\{0^\circ, 90^\circ, 180^\circ, 270^\circ\}$  while the outer 12 elements (also clockwise) are driven with  $30^\circ$  increments  $\{0^\circ, 30^\circ, \dots, 270^\circ, 330^\circ\}$ . This creates a destructive field pattern on the longitudinal axis of the array because elements opposite from each other are driven out of phase. Other patterns are created by varying the phase increment in the rotation or by adjusting the element phases across any axis to create destructive interference (see Table I for the phase distributions of the patterns in Fig. 2). This technique has been shown to decrease the required treatment time for a single sonication of a multiple focus pattern as

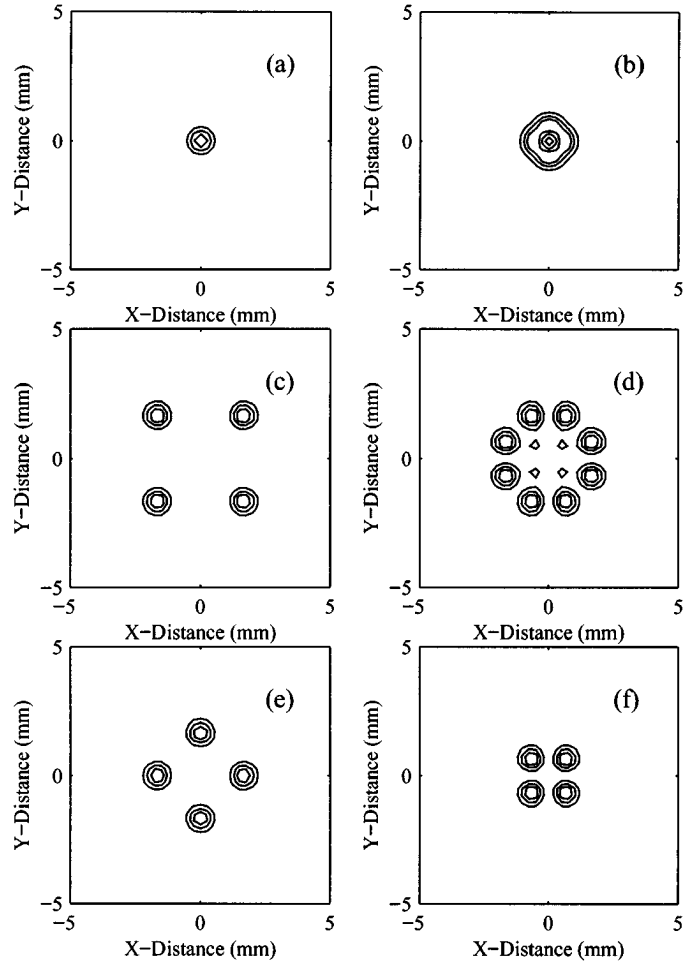


Fig. 2. Simulated fields for optimization generated using the mode scanning technique [21].

TABLE I

THE ELEMENT PHASES (IN DEGREES) USED TO CREATE THE FIELD PATTERNS FOUND IN FIG. 2 (SEE FIG. 1 FOR ELEMENT NUMBERING).

Element (Fig. 1)	(a)	(b)	(c)	(d)	(e)	(f)
1	0	90	0	0	0	180
2	0	120	180	270	270	180
3	0	150	0	90	0	0
4	0	180	180	180	270	0
5	0	60	180	90	90	180
6	0	90	0	180	180	180
7	0	180	180	0	90	0
8	0	210	0	270	180	0
9	0	30	0	270	0	0
10	0	0	180	0	270	0
11	0	270	0	180	0	180
12	0	240	180	90	270	180
13	0	0	180	180	90	0
14	0	330	0	90	180	0
15	0	300	180	270	90	180
16	0	270	0	0	180	180

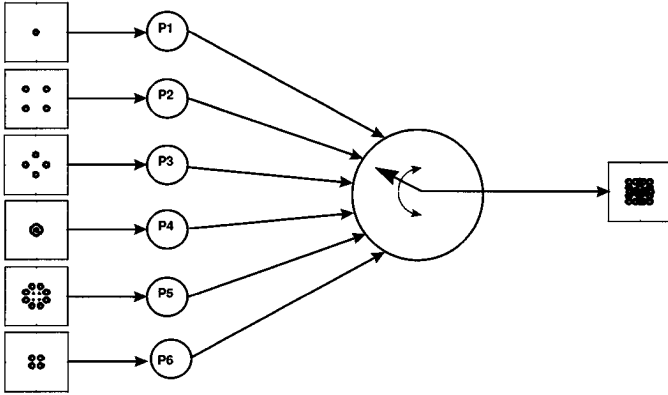


Fig. 3. Switching technique diagram. On the left are the pressure plots for the six input patterns. The power levels for these patterns (P1-P6) are determined through a gradient optimization and rapid switching is then used to create an effective field as seen on the right.

compared to other methods of pattern synthesis [11]. The patterns were selected so there was a distribution of foci throughout the proposed treatment volume without extensive sidelobes (greater than 10% of desired foci) outside of the three dimensional region of interest.

Fig. 3 illustrates how the six patterns were used in the switching technique. Basically, the driving signals rapidly changed between the six input fields to imitate a continuous wave (CW) signal with more uniformly dispersed power in the region of interest. The power levels for each individual field (P1-P6) were determined using a direct-weighted gradient search routine (50 iterations) [22] to find the “global” minimum of a mean-squared cost function comparing the simulated dose ( $D_{sim}$ ) to a uniform thermal dose ( $D_{ideal}$ ) over a region ( $V$ ) slightly larger than the power deposition patterns.

$$C_f = \sqrt{\iiint_V (D_{sim}(x, y, z) - D_{ideal}(x, y, z))^2}. \quad (1)$$

In this case the region had a volume of  $0.6 \times 0.6 \times 1.0 \text{ cm}^3$ . The ideal thermal dose of 5000 equivalent minutes at  $43^\circ\text{C}$  was chosen so the threshold value for tissue necrosis (240 equivalent minutes) [20] was exceeded by a factor of 20, thus reducing the chance of nonnecrosed tissue within the region of interest. The switched sonication duration was set at 10 seconds so the simulations matched the time necessary for the MRI to gather several temperature images during the heating cycle (longer sonications were avoided to decrease perfusion dependence [23]). Several minutes passed between consecutive sonications to avoid any effects of near field heating.

#### E. Switching Rate

Theoretical simulations were performed to find the effect of switching rate on the effective dose distribution. To accomplish this task, the dose field was calculated for a 10 second sonication which consisted of various switching cycle times ranging from 50 to 900 ms for six and for three

input fields (the cycle time is defined as the time to cycle through all of the input fields once). The results of the simulation were then compared to a simulation which had as its input an arithmetically averaged power deposition pattern which was created by directly weighting the previously cycled input fields. The goal of this study was to find the theoretical effect of the hardware switching limitation speed on the generation of an effective continuous wave field.

#### F. Experimental Set Up Using MRI Thermometry

The phased array was placed in a submerged 3-dimensional positioning system within a clinical 1.5 T Signa MRI (both GE Medical Systems, Milwaukee, WI) for sonication on the thigh muscle of four New Zealand white rabbits in vivo [25]. For each rabbit, the thigh was situated at the natural focus of the array and a series of higher power sonications both with and without pattern switching were performed while obtaining temperature sensitive images [15], [24]. These images used a fast spoiled gradient echo sequence with repetition time  $TR = 26.1 \text{ ms}$ , echo time  $TE = 12.8 \text{ ms}$ , flip angle  $= 30^\circ$ , bandwidth  $= 7.2 \text{ kHz}$ , resolution  $128 \times 256$ , field of view  $FOV = 16 \text{ cm}$ , and slice thickness  $= 3 \text{ mm}$ . The time to obtain a single temperature image was 3.3 seconds and some temperature elevation occurred during data acquisition. The time sequence of images included a single image taken pre-sonication, three images during the 10 second heating, and six images during the 20 second post-sonication cooling period. After the temperature sensitive images were obtained, proton density and T2 weighted images (fast spin echo sequence with  $TR = 2000 \text{ ms}$ ,  $TE = 17$  and  $68 \text{ ms}$ , echo train length  $= 8$ ,  $FOV = 16 \text{ cm}$ , slice thickness  $= 3 \text{ mm}$ ) were taken to demarcate the lesion areas and evaluate treatment execution.

### III. RESULTS

#### A. Simulation and Water Scanned Comparison of Array Fields

Phased array operation was initially tested by scanning the transducer in a water bath. Fig. 4 compares a few of the theoretical and experimental scans. The four foci pattern which forms a box in the focal plane demonstrates the off-axis spatial limits of power deposition for this given array geometry; therefore, outlining the maximum volume which can be necrosed without physically moving the transducer. Discrepancies in the focal width between the simulated and scanned results may be attributed to transducer element misalignment and the relatively large thermistor cross-section (0.25 mm). The temporal switching operation of the hardware was confirmed by slowly switching between the different multiple focus fields with the focal plane of the transducer located at the surface of the water bath.

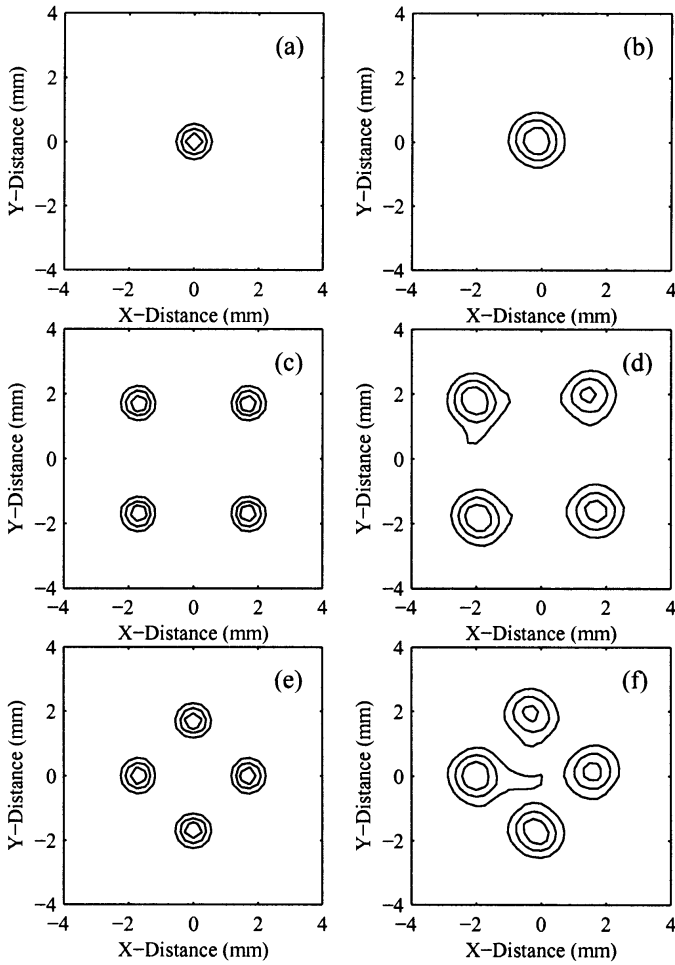


Fig. 4. Simulated and water scanned fields for 16 element phased array (a, c, e theoretical; b, d, f experimental).

TABLE II  
OPTIMIZED SWITCHING POWER LEVELS.

Acoustic pattern: Fig. 2	Optimized power (W)
(a)	3
(b)	1
(c)	99
(d)	83
(e)	46
(f)	1

*B. Optimization Results*

The optimized power levels for the six patterns in Fig. 2 are listed in Table II. There are two main results of the optimization. First, the optimized power levels for each field did not directly correspond to the number of foci of that given field. This is due to an uneven overlap between the temperature and dose responses to the different power deposition fields. Second, the optimal driving powers for three of the patterns {c, d, e} were much larger than the other three patterns {a, b, f} such that the less substantial patterns could be eliminated.

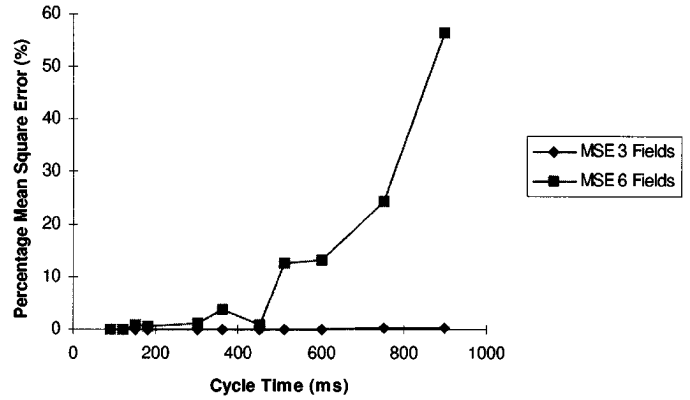


Fig. 5. Normalized mean square error plots for cycle times comparing the temporally switched “effective” field to the theoretical fields produced by an input field formed by arithmetically averaging the three or six input fields, respectively. The error was normalized by dividing it by the optimal dose level.

From a practical standpoint, reducing the number of switched fields is advantageous because there is a limitation on how fast the hardware can toggle between various phase and power patterns: 10 Hz was the limitation switching speed of the system used in this research (the minimum sonication time per field was 100 ms). In order to create an “effective” field which represents an arithmetic average of temporally switched fields as if the field were CW, the switching frequency must become very fast as the number of fields increases (see Fig. 5). For example, to avoid large errors between the “effective” dose response produced by temporal switching and the theoretical dose response from the average of the six input fields, the fields must be cycled faster than 600 ms (the cycle time is defined as the time to cycle through all of the input fields once). This exceeds the switching rate of the hardware. The three fields, however, require a cycle time below the hardware limitation.

The simulated thermal dose for the optimized switching pattern and a non-switched pattern [pattern (c) of Fig. 2] of the same average power is found in Fig. 6. It is clear from the simulation that the nonswitched pattern yields much higher peaks and lower dips in thermal dose within the region of interest. One can also see that the switching technique should create a contiguous lesion while the nonswitched foci of the same power would leave a center volume of nonnecrosed tissue—an undesirable feature when treating a large volume tumor. In order to create a completely necrosed region using a simple four focus pattern, the power and postsonication wait duration must be increased more than 20% as listed in Table III.

Simulations with varying biological parameters tested the switching technique under higher perfusion and tissue inhomogeneities. First, the simulated perfusion was increased from 1 kg/m<sup>3</sup>s to 10 kg/m<sup>3</sup>s. For a static sonication of 49 W, the dose at its center decreased from 265 equivalent minutes at 43°C to 90 equivalent minutes, indicating that even more power would be necessary to cause a continuous necrosis (Fig. 7). The center dose of the 38 W switching technique also dropped but the complete volume

TABLE III

COMPARISON OF SWITCHED VS. NONSWITCHED FIELDS TO PRODUCE A CONTINUOUS LESION OF 240 EQUIVALENT MINUTES DOSE AT 43°C.

	Non-switched pattern (b)	Switched pattern
Average power	49 W	38 W
Treatment duration	71 s	59 s
Peak temperature	71°C	58°C

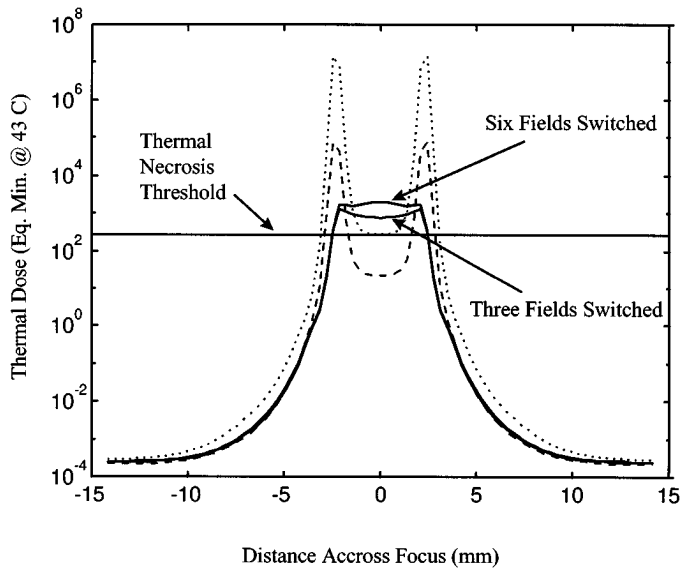


Fig. 6. Optimization results of simulated dose across the focal axis. The four lines correspond to the thermal dose delivered using a simple four focus pattern at 38 W (dashed), a four focus pattern at 49 W (dotted), a switched pattern at 38 W using all 6 fields (solid), and a switched pattern at 38 W using the three most significant fields (solid).

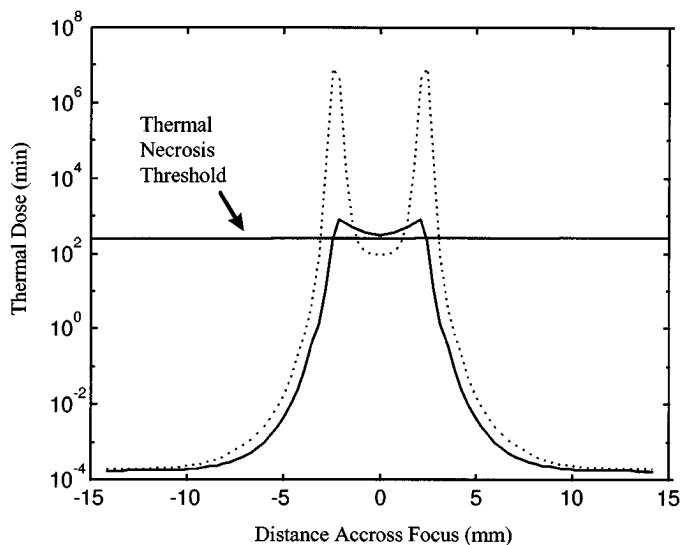


Fig. 7. High perfusion simulation results ( $10 \text{ kg/m}^3 \text{ s}$  vs.  $1 \text{ kg/m}^3 \text{ s}$  in Fig. 6). The 49 W static sonication (dotted) dips below the necrosis threshold while the 38 W switched sonication (solid) still creates a continuous necrosis region.

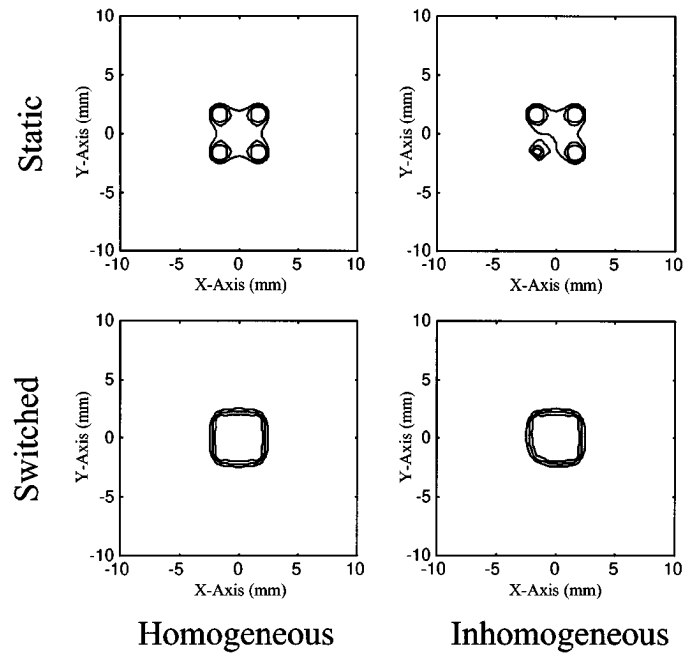


Fig. 8. Comparison of homogeneous tissue and homogenous tissue with a small section of 80% SAR at lower left foci. Contour lines correspond to dose of 15, 60, and 240 minutes for 38 W average sonications.

still exceeded the 240 minute threshold (also Fig. 7). Second, inhomogeneous tissue was modeled by creating a low absorption area (80% absorption as compared to rest of tissue) with a cross-section of  $0.75 \times 0.75 \text{ mm}$  at the location of one of the foci for the static and switched fields. The cross axial dose contours are graphed in Fig. 8. The switched contour exhibits a small decrease on the outer corner of the necrosed region while the nonswitched necrosis experiences a dip in thermal dose within its outer borders.

### C. MRI Experimental Results

Fig. 9 contains the temperature contour plots experimentally obtained using MRI through the focal plane of a switched sequence sonication and a single four focus sonication [pattern (c) of Fig. 2] of the same average power (76 W). One can see from the two plots that the temperature distribution is more uniform for the switched pattern than for the simple four focus pattern. Specifically, the center of the four focus pattern was thermally "filled in" by switching between multiple focus patterns instead of relying on thermal conduction from the four distant outer foci.

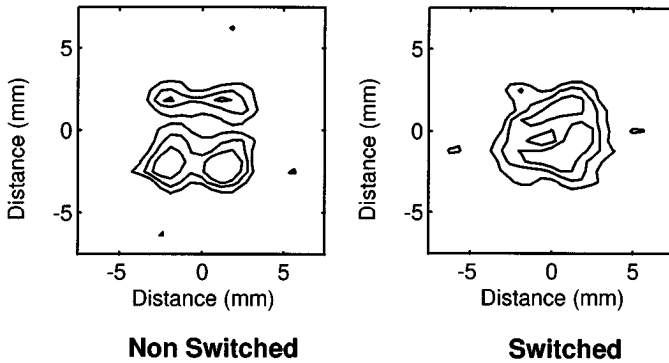


Fig. 9. In vivo thermal contour images for (left) nonswitched and (right) switched sonications (contour lines at 10, 15, and 20°C temperature increases) measured using MRI.

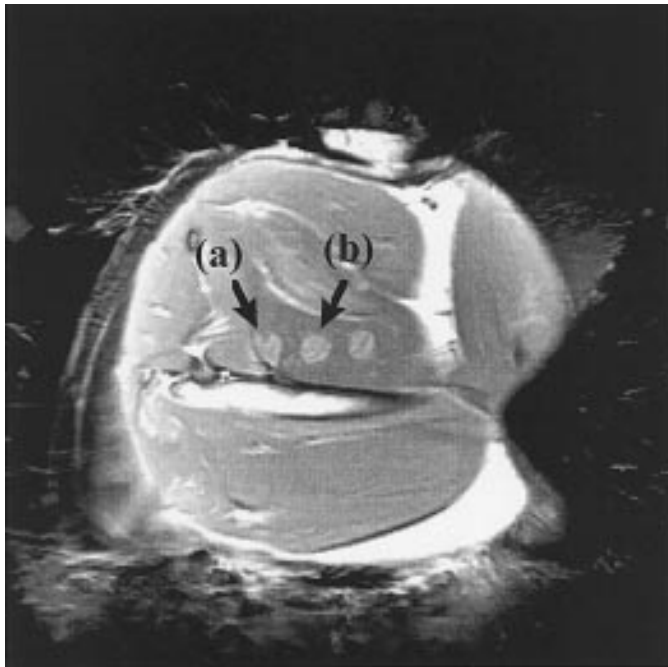


Fig. 10. Proton density weighted image of thermal necrosis caused by (a) single four focus pattern and (b) switched focus pattern across axis.

Both sonications yielded continuous lesions as determined in postsonication images (Fig. 10).

To show that the switched fields could produce continuous lesions at lower powers than a simple multiple focus pattern, a second set of 10 second sonications at 68 W were performed. Fig. 11 was obtained after these lower power sonications. Note that the switched pattern completely coagulated the treatment volume while the multiple focus pattern left an unaffected region in its center. This response may be better explained by considering the temperature profiles across the sonication regions during treatment (Fig. 12). The switched pattern yielded a more uniform temperature distribution and overall lower peak temperature than the single multiple focus pattern as seen in simulations.

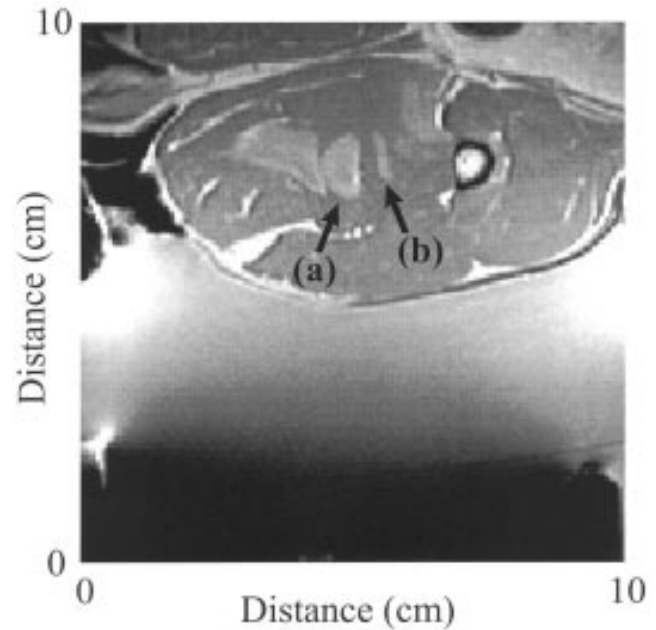


Fig. 11. Proton density weighted image of lesions produced using 68 W average power: (a) switched pattern lesion and (b) nonswitched pattern lesion.

#### IV. DISCUSSION

The main goal of this research is to use pretreatment optimization to improve and experimentally implement the use of temporal switching for a phased array. As a part of this goal, this research presents the first quantitatively measured implementation of a temporally switched ultrasound surgery treatment in vivo. Unlike previous switching techniques, this research did not implement temporal switching only to increase the effective focal volume of an array, but also to improve the treatment conditions such as cooling duration, average power, and peak temperature. The simulation and in vivo results indicate that this goal can be accomplished: temporally switched fields can decrease peak temperature and create regions of necrosis at lower average powers than nonswitched fields.

A second advantage of optimizing power among a set of deposition patterns is to reveal those patterns which have the greatest effect on the thermal dose delivered to a given volume. By indicating fields which have lesser effects, a smaller set of fields can be implemented such that the required switching rates are not excessively fast. As is expected, an “average” or effective field can be produced at lower switching rates when fewer fields are used. A switching frequency of 10 Hz was fast enough to produce an effective average field as described in [13] for three fields but not for six. Therefore, given the hardware limitation, it is preferable to switch between the smaller number of fields as long as the deletion of fields from the larger set does not cause a drastic deviation from the ideal dose response of the complete set.

A third advantage to pretreatment optimization is the indication of power levels that are not necessarily depen-

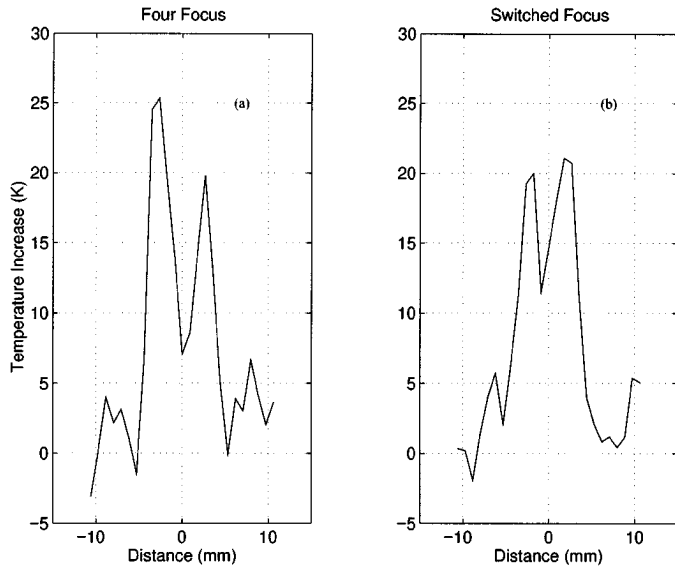


Fig. 12. Temperature response across 68 W average sonications in vivo measured using MRI: (a) four focus pattern and (b) switched focus pattern

dent on the number of foci within the pattern. The precise power levels of a set of patterns, however, is somewhat forgiving. A variation of powers using the set  $\{(c), (d), (e)\}$  of Fig. 2 was found to yield similar thermal and dose responses close to the global minimum. Not surprisingly, therefore, the choice of deposition patterns appears to be the most critical feature when designing a treatment—the gradient search having the ability to highlight those patterns of greatest utility and to indicate the relative power levels for those patterns. These levels can then be proportionally scaled for in vivo treatments which may have varying or unknown tissue absorption.

The temporal switching tested in this research could possibly be further improved in two ways. First, the results presented in this paper were all performed for a 10 second sonication so that the theoretical and experimental results could be compared (the limitation being the image access time of the MRI). The optimization would, therefore, have to be repeated for a different sonication times to correctly optimize the relative power levels. The sonication time was not optimized. Second, a variation of the switching technique would optimize both the choice of field and its relative power for each time segment in the switching period, imitating an adaptive power feedback control. In such a case, the use of an ideal “arithmetic average” field as an “effective” field may not be desirable because the power levels for each individual field would vary during the sonication duration.

Both simulated and experimental results indicate that another reason to use temporally switched fields is to decrease the dependency of tissue inhomogeneity and biological parameters. This is due to the fact that the switching technique distributes power over a larger volume than the small number of concentrated foci from a static pattern. For example, in the simulation of the inhomogeneous

tissue the static dose response dropped more quickly between the four outer foci than did the dose response of the switched dose pattern (Fig. 8). Various samples of in vivo sonications in this research also demonstrated that the dependency of tissue homogeneity may not be as great when switching is used instead of static sonication (as an example, one of the foci in the static sonication of Fig. 11 is greatly reduced). It is hypothesized that a more uniform power deposition decreases the chance that a temperature sink such as a blood vessel will seriously effect the treatment when it spatially overlaps with one of the static foci as described in [23]. Therefore, while the ability to spread power distribution in ultrasound surgery over a large number of foci has previously been found to be preferable from a treatment time consideration [4], [5], it may also be preferable to ensure treatment operation.

Lastly, this research again showed that magnetic resonance imaging is a powerful tool to detect thermal increases in vivo noninvasively. In particular, the temperature images demonstrate the ability of MR imaging to detect thermal increases of temporally switched fields, illustrating the feasibility of real time monitoring of a dynamically changing sonication pattern. This has important implications toward real time monitoring of ultrasound surgery.

## REFERENCES

- [1] C. A. Cain and S. Umemura, “Concentric ring and sector-vortex phased-array applicators for ultrasound hyperthermia,” *IEEE Trans. Microwave Theory Tech.*, vol. MTT-34, no. 5, pp. 542–551, 1986.
- [2] E. S. Ebbini and C. A. Cain, “Multiple-focus ultrasound phased-array pattern synthesis: optimal driving-signal distributions for hyperthermia,” *IEEE Trans. Ultrason., Ferroelect., Freq. Contr.*, vol. 36, no. 5, pp. 540–548, 1989.
- [3] X. Fan and K. Hynynen, “Control of the necrosed tissue volume during non-invasive ultrasound surgery using a 16-element phased array,” *Amer. Assoc. Phys. Med.*, vol. 22, no. 3, pp. 297–308, 1995.
- [4] —, “A study of various parameters of spherically curved phased arrays for noninvasive ultrasound surgery,” *Phys. Med. Biol.*, vol. 41, pp. 591–608, 1996.
- [5] H. Wan, P. Van Baren, E. S. Ebbini, and C. A. Cain, “Ultrasound surgery: comparison of strategies using phased array systems,” *IEEE Trans. Ultrason., Ferroelect., Freq. Contr.*, vol. 43, no. 6, pp. 1085–1098, 1996.
- [6] C. Damianou and K. Hynynen, “Focal spacing and near-field heating during pulsed high temperature ultrasound therapy,” *Ultrason. Med. Biol.*, vol. 19, no. 9, pp. 777–787, 1993.
- [7] K. Hynynen, A. Darkazanli, E. Unger, and J. F. Schenck, “MRI-guided noninvasive ultrasound surgery,” *Med. Phys.*, vol. 20, no. 1, pp. 107–115, 1993.
- [8] K. Hynynen, “The threshold for thermally significant cavitation in dog’s thigh muscle in vivo,” *Ultrason. Med. Biol.*, vol. 17, pp. 157–169, 1991.
- [9] A. Sibille, F. Prat, J.-Y. Chapelon, F. A. E. Fadil, L. Henry, Y. Theillere, T. Ponchon, and D. Cathignol, “Characterization of extracorporeal ablation of normal and tumor-bearing liver tissue by high intensity focused ultrasound,” *Ultrason. Med. Biol.*, vol. 19, no. 9, pp. 803–813, 1993.
- [10] A. L. Malcolm and G. R. ter Haar, “Ablation of tissue volumes using high intensity focused ultrasound,” *Ultrason. Med. Biol.*, vol. 22, no. 5, pp. 659–669, 1996.
- [11] X. Fan and K. Hynynen, “Ultrasound surgery using multiple sonications—treatment time considerations,” *Ultrason. Med. Biol.*, vol. 22, no. 4, pp. 471–482, 1996.

- [12] S. Umemura and C. A. Cain, "The sector-vortex phased array: acoustic field synthesis for hyperthermia," *IEEE Trans. Ultrason., Ferroelect., Freq. Contr.*, vol. 36, no. 2, pp. 249–257, 1989.
- [13] E. S. Ebbini and C. A. Cain, "Optimization of the intensity gain of multiple-focus phase array heating patterns," *International Journal of Hyperthermia*, vol. 7, no. 6, pp. 953–973, 1991.
- [14] R. Seip, P. Van Baren, C. A. Cain, and E. S. Ebbini, "Non-invasive real-time multipoint temperature control for ultrasound phased array treatments," *IEEE Trans. Ultrason., Ferroelect., Freq. Contr.*, vol. 43, no. 6, pp. 1063–1073, 1996.
- [15] K. Kuroda, K. Abe, S. Tsutsami, Y. Ishihara, Y. Susuki, and K. Sato, "Water proton magnetic resonance spectroscopic imaging," *Biomed. Thermol.*, vol. 13, pp. 43–62, 1993.
- [16] E. S. Ebbini and C. A. Cain, "A spherical section ultrasound phased array applicator for deep localized hyperthermia," *IEEE Trans. Biomed. Eng.*, vol. BME-38, no. 7, pp. 634–643, 1991.
- [17] H. F. Stewart, "Ultrasonic measurement techniques and equipment output levels," *Essentials of Medical Ultrasound: A Practical Introduction to the Principles, Techniques, and Biomedical Applications*, pp. 77–116, 1982.
- [18] J. Zemanek, "Beam behavior within the nearfield of a vibrating piston," *J. Acoust. Soc. Amer.*, vol. 49, no. 1, pp. 181–191, 1971.
- [19] H. H. Pennes, "Analysis of tissue and arterial blood temperatures in the resting human forearm," *J. Appl. Phys.*, vol. 1, pp. 93–122, 1948.
- [20] S. Separeto and W. Dewey, "Thermal dose determination in cancer therapy," *Int. J. Radiat. Oncol. Biol. Phys.*, vol. 10, pp. 787–800, 1984.
- [21] R. J. McGough, H. Wang, E. S. Ebbini, and C. A. Cain, "Mode scanning: a heating pattern with ultrasound phased arrays," *International Journal of Hyperthermia*, vol. 10, no. 3, pp. 433–442, 1994.
- [22] R. L. Zahradnik, *Theory and Techniques of Optimization for Practicing Engineers*. New York: Barnes & Noble, 1971.
- [23] L. N. Dorr and K. Hynynen, "The effect of tissue heterogeneities and large blood vessels on the thermal exposure induced by short high-power ultrasound pulses," *Int. J. Hyperthermia*, vol. 8, no. 1, pp. 45–59, 1992.
- [24] A. H. Chung, K. Hynynen, V. Colucci, K. Oshio, H. E. Cline, and F. A. Jolesz, "Optimization of spoiled gradient-echo phase imaging for in vivo localization of a focused ultrasound beam," *Magn. Resonance Med.*, vol. 36, pp. 745–752, 1996.
- [25] K. Hynynen, W. R. Freund, H. E. Cline, A. H. Chung, R. D. Watkins, J. P. Vetro, and F. A. Jolesz, "A clinical, noninvasive MR imaging-monitored ultrasound surgery method," *Radiographics*, vol. 16, pp. 185–195, 1996.

**Douglas R. Daum** was born in Wilmington, DE, on December 29, 1968. He received the B.S. and M.S. degrees in electrical engineering from Brigham Young University in 1993 and 1994, respectively. He is currently a candidate for the Ph.D. degree in medical engineering in the Harvard/M.I.T. Division of Health Sciences and Technology, Cambridge, MA.

His current research interests are in the therapeutic application of phased array ultrasound.